ELSEVIER

Journal of Alloys and Compounds 356–357 (2003) 211–217

Journal of ALLOYS AND COMPOUNDS

www.elsevier.com/locate/jallcom

Structure and bonding in YH_x as derived from elastic and inelastic light scattering

J. Schoenes*, A. Borgschulte, A.-M. Carsteanu, H. Kierey, M. Rode

Institut für Halbleiterphysik und Optik, Technische Universität Braunschweig, Mendelssohnstrasse 3, D-38106 Braunschweig, Germany

Received 1 September 2002; accepted 15 November 2002

Abstract

The optical properties in the visible and infrared (IR) as well as the Raman effect are reported for thin films of YH_x with $2 \leq x \leq 3$. From an analysis of the IR spectra, the Szigeti effective charges have been derived. It is found that in the insulating γ phase ($x \approx 3$) hydrogen is negatively charged with a transfer of about 0.5 e to every hydrogen atom. Raman scattering spectra display one line in YH_2 and up to 13 lines in YH_3. A comparison with spectra of deuterated samples allows to identify hydrogen vibrations. An analysis of the polarization dependence evidences that the structure is non-centrosymmetric. The results support models for the electronic structure which assume strong electron correlations.

Keywords: Thin films; Vapor deposition; Crystal structure and symmetry; Light absorption and reflection; Inelastic light scattering

1. Introduction

Although electrical transport experiments performed since the mid 1950s [1,2] indicated a hydrogen induced metal–insulator transition on loading rare-earth metals and early reemission measurements on $EuH_{2-\delta}$ powders gave evidence for a gap of 1.85 eV [3], it took until the discovery of the switching properties of Y and La hydride films in 1996 [4] that the striking optical properties of rare-earth hydrides were more widely recognized. Since that time several studies of the optical properties of thin films in the visible spectral range have been performed. Some more applied work focus on the optimization of the transmittance [5], other more basic work concentrates on the size and the energy dependence of the gap to unravel the electronic structure [6]. To deploy its full power, optical spectroscopy requires samples with surfaces which are flat and perfect on the scale of about one tenth of the wavelength [7]. Therefore, powder samples are not suited, while thin films are optimal, unless they deteriorate under the ambient conditions of the measurement. Complications can also occur if the films have to be covered with protective layers and/or the substrate contributes to the result of the measurement. This is the case in general for rare-earth hydrides, in which often a Pd cap layer is used to protect the metal against oxidation and to dissociate H_2 into atomic hydrogen. Even for a Pd cap layer as thin as 5 nm the absorption is non-negligible compared to that for potential indirect or dipole-forbidden direct transitions at the gap of an insulator and this renders difficult, if not impossible, the exact determination of the energy dependence of the absorption near the fundamental gap [6]. Therefore, we have chosen not to study the electronic structure by optical investigations near the gap, but to address some of the open questions through an investigation of the ionicity of the compound. This is done by a quantitative determination and analysis of the complex dielectric function on both sides of the one-phonon excitations. Besides these results for elastic interaction of light with matter, we also review the state of the art of the study of the phonons in hydrides using inelastic light scattering. From the polarization and angular dependence of the Raman spectra, conclusions about the symmetry of the crystal structure can be drawn, which are particularly valuable, since neutron scattering is not very suitable to study hydrides and even deuterides. Some of the data have been published recently [8,9], others are presented for the first time.

*Corresponding author. Tel.: +49-531-391-5130; fax: +49-531-391-5155.

E-mail address: j.schoenes@tu-bs.de (J. Schoenes).

0925-8388/03/$ – see front matter
doi:10.1016/S0925-8388(03)00109-9

2. Experimental procedure

The metallic cap layer prevents the usual optical techniques to be applied. In particular Raman effect measurements can not be performed through the metallic cap. Therefore, it is essential to deposit the switchable mirror on a transparent substrate. Polycrystalline films of yttrium can be obtained by evaporation onto glass or quartz substrates. However, the transmission of these substrates in the IR is very limited. To perform transmission or reflectivity measurements from the substrate side in the IR, we have used silicon substrates. Although these are (100) oriented single crystalline wavers, the films are not epitaxial, but [0001] textured. Epitaxial Y films can be grown on (111) oriented CaF_2 [10] and BaF_2 [11] substrates. The transmission of these substrates is limited in the IR to approximately 1100 and 900 cm^{-1}, respectively. On the high photon energy side the transmission range of these earth-alkali halogenides extends far above the visible spectral range making them very suitable for studies using the green argon laser line at λ=514.5 nm. Fig. 1 (top) shows reflection high energy electron diffraction (RHEED) patterns taken at different stages of the growth of yttrium on CaF_2 (111) substrates. For this film grown at 700 °C in our molecular-beam epitaxy system (MBE) in a vacuum of 10^{-10} mbar we find a Volmer–Weber type of growth. The sharp streaks, Kikuchi lines and Laue circles for the film thickness of 200 nm indicate a good crystallinity and atomic flat surfaces. There is a lattice-parameter mismatch of 6% between the CaF_2 substrate and bulk Y. As can be derived from the densitometer scan of the RHEED pattern (Fig. 1, bottom) our Y film has a lattice parameter which is 8.5% smaller than that of the substrate. We attribute this somewhat increased misfit to the interfacial reaction between Y and F from the CaF_2 substrate [12].

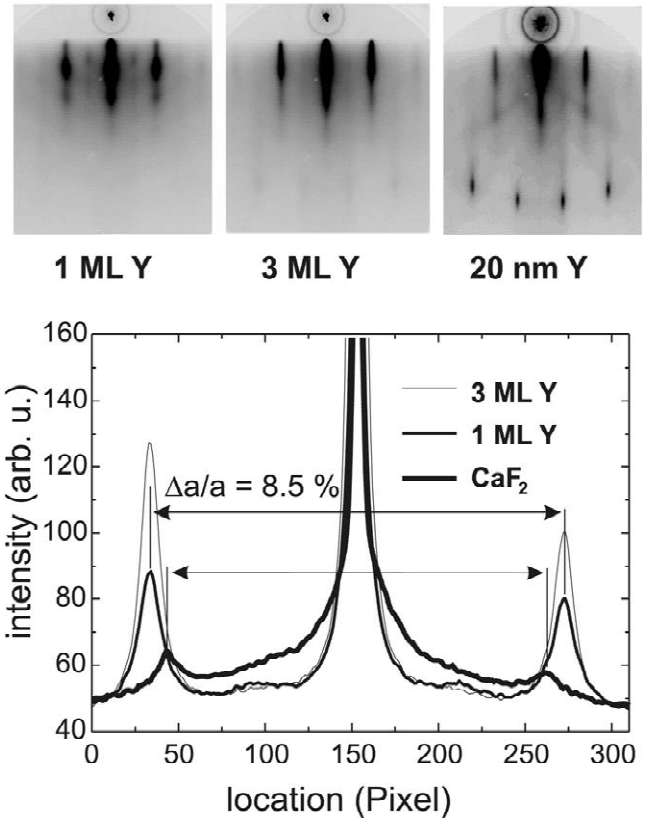

Fig. 1. RHEED patterns taken at various stages of the growth of an yttrium film on a (111)-oriented CaF_2 substrate (top) and intensity scans through the RHEED patterns for the substrate and the one and three monolayer thick Y film (bottom). Note that already the one monolayer thick Y film has the lattice parameter of the thick film.

For the IR transmission measurements films of various thickness have been used. In particular, two Y films with different thickness d_1 and d_2 but with the same cap layer were deposited on the very same substrate. By dividing the intensity transmitted by the thicker film (say d_1) by that of the thinner film (say d_2), the effect of the cap layer drops out and one obtains $I_1/I_2=\exp[-K(d_1-d_2)]$, where K is the absorption of the film material under investigation. The transmission measurements have been performed with a Bruker 113v Fourier transform spectrometer in the range of 300 to 6000 cm^{-1} (0.0372–0.744 eV). In addition, using a Perkin-Elmer 551S UV–Vis spectrophotometer, transmission as well as reflectivity measurements have been carried out from 12 500 to 25 000 cm^{-1} (1.55–3.10 eV) to derive the refractive index in the transparent regime of YH_3 from interference effects. For the Raman effect measurements two set-ups have been used. With a conventional laboratory-built system consisting of a triple grating polychromator, a liquid nitrogen cooled CCD camera, a helium cryostat and an Ar^+ laser operated at 600 mW most of the data have been collected. This system integrates over a sample area of about 1 mm^2. Since the depth of focus is quite low the scattered light does not come only from the thin film but also from the CaF_2 or BaF_2 substrate through which the light falls onto the sample. The second system is a commercial micro-Raman spectrometer (Jobin Yvon LabRam HR) operated with a diode-pumped Nd:YAG laser of 150 mW. The light beam of 532 nm wavelength is focused with a microscope on an area of a few μm^2, the exact size depending on the focal length of the microscope objective. The confocal system allows largely to avoid contributions in the scattered light from the substrate, giving to the spectra a much flatter background.

3. One-phonon excitations and Szigeti effective charge

The excitation of one-phonon modes with electromagnetic radiation requires the presence of an electric dipole moment [13]. As a consequence, except for very special cases, phonons can not be studied in metals [14]. Therefore, our IR investigations concentrate here on the insulating $YH_{3-\delta}$ phase. Fig. 2 shows the intensity ratio I_1/I_2 of the light transmitted through films with original Y thick-

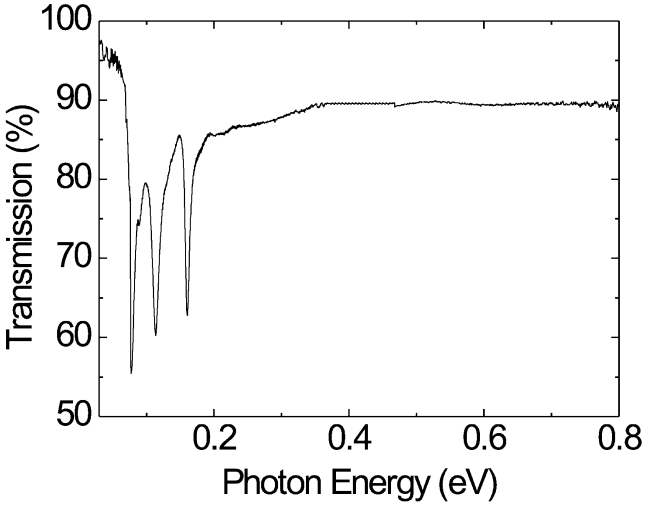

Fig. 2. Transmission curve derived from the ratio of the transmission of two YH_3 films with different thickness deposited on the same silicon substrate. $T=300$ K, $d_{eff}=92$ nm.

ness $d_1=200$ and $d_2=120$ nm[1] sandwiched between the Si substrate and the Pd cap layer. We find three strong and two weak lines[2], which we assign to the excitation of transverse optical phonons. This interpretation is substantiated by the substitution of deuterium for hydrogen. As shown in Fig. 3 for another film grown epitaxially on CaF_2, such a substitution shifts the phonon peaks to lower frequency by a factor very close to $\sqrt{2}$. This indicates that for these phonon modes the hydrogen, respectively, the

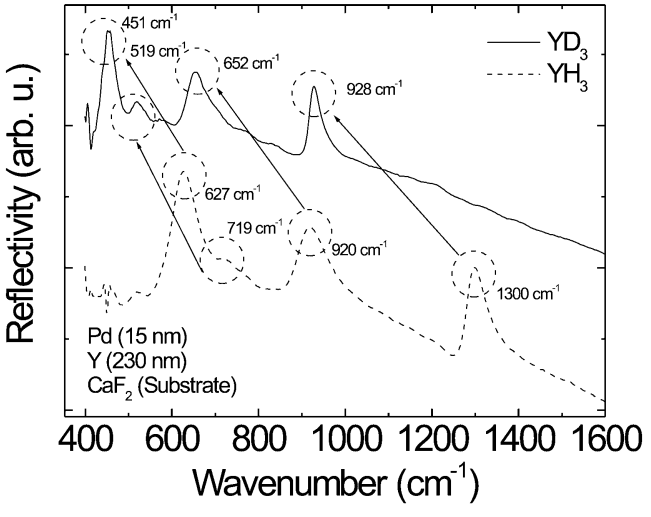

Fig. 3. Shift of the phonon peaks on substitution of deuterium for hydrogen. The reflectivity spectra have been taken through the Pd-cap layer. Note that maxima in the reflectivity are shifted compared to maxima in the optical conductivity spectra.

[1]On hydrogenation the film thickness increases by 15.9%.

[2]The weak lines are on both sides of the strong line with the lowest energy. They appear more clearly in the optical conductivity or the energy loss [8].

deuterium sublattice vibrates. The symmetry of the lattice determines the number of IR-active phonon modes. As will be discussed in detail after the presentation of the Raman-scattering results, one can already exclude on the basis of the observed five IR-active phonon modes that YH_3 crystallizes in the simple hexagonal $P6_3mmc$ structure.

To derive the exact frequencies of the transverse optical phonons, one needs to compute the real part of the optical conductivity. The frequencies of the longitudinal optical phonons follow from the maxima in the energy loss spectrum $\mathrm{Im}[-1/\varepsilon(\omega)]$ [13], where $\varepsilon(\omega)=\varepsilon_1(\omega)+i\varepsilon_2(\omega)$ is the complex dielectric function with its real part $\varepsilon_1(\omega)=n(\omega)^2-k(\omega)^2$ and its imaginary part $\varepsilon_2(\omega)=2n(\omega)\cdot k(\omega)$. Here $n(\omega)$ and $k(\omega)$ are the refractive and the absorption index, respectively. The latter is related to the measured absorption constant $K(\omega)$ by the relation $k(\omega)=K(\omega)\cdot\lambda_{vac}/4\pi$, where λ_{vac} is the wavelength of light in vacuum. To obtain $n(\omega)$ we use the Kramers–Kronig relation between $n(\omega)$ and $k(\omega)$:

$$n(\omega)=1+\frac{2}{\pi}\cdot P\int_0^{\infty}\frac{\omega' k(\omega')}{\omega'^2-\omega^2}\mathrm{d}\omega' \tag{1}$$

where P is the principle value. Since we know $k(\omega')$ only over a restricted frequency range we use a trick and divide up the integral over ω' from 0 to ∞ into two parts:

$$n(\omega)=\frac{2}{\pi}\cdot P\int_0^{\omega_c}\frac{\omega' k(\omega')}{\omega'^2-\omega^2}\mathrm{d}\omega'+\frac{2}{\pi}\cdot P\int_{\omega_c}^{\infty}\frac{\omega' k(\omega')}{\omega'^2-\omega^2}\mathrm{d}\omega'+1 \tag{2}$$

The first part extends over the one-phonon-excitation range and has been measured. The second part extends over the interband transitions above the gap energy. This integral of $k(\omega')$ over the interband transitions (plus 1) gives the refractive index in the transparent range below the absorption edge which we call n_{opt}. It can be determined, if the film thickness is known, from the extrema of the reflectivity and transmission spectra arising from interferences on the transparent film. Fig. 4 displays such spectra for an YH_3 film of 280 nm thickness grown on a CaF_2 substrate and capped with a 15 nm thick Pd layer. The fits allow also for some weak absorption, so that $k(\omega)$ and consequently $\varepsilon_2(\omega)$ are not zero. The resulting $\varepsilon_1(\omega)$ and $\varepsilon_2(\omega)$ spectra (Fig. 5) show the expected weak energy dependence and the value for $\varepsilon_1(\omega)$ is similar to results from ellipsometry [6]. With the derived $n_{opt}=2.8$ the Kramers–Kronig transformation can now be performed leading to all optical functions in the IR. A fit of the optical conductivity spectrum $\sigma_1(\omega)=\omega\cdot\varepsilon_2(\omega)/4\pi$ with five Lorentzians for the phonons and a small Drude term for the free carriers present at room temperature leads to the five transverse optical phonon frequencies ω_{TO}, expressed in wave numbers $\nu=\omega/2\pi c$: 609, 620, 713, 896 and 1282 cm^{-1}. The same fit for the energy loss function

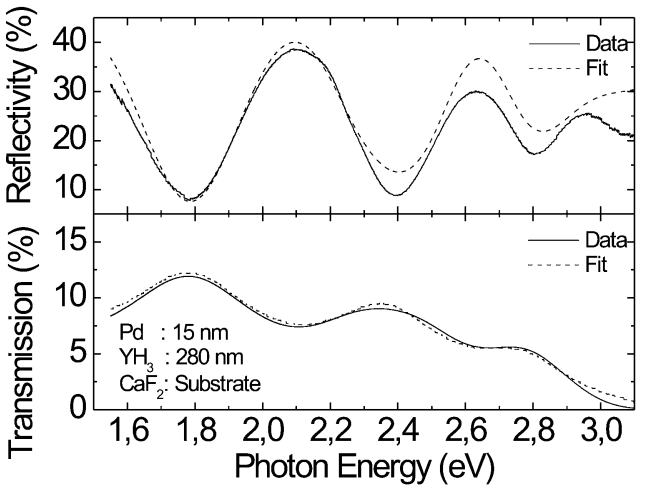

Fig. 4. Reflectivity (top) and transmission spectra (bottom) in the transparent spectral range of YH_3 measured from the substrate side. The modulations are due to interference.

gives for the longitudinal phonon modes the wave numbers: 695, 770, 831, 1093 and 1353 cm^{-1}. These values can be incorporated into the generalized Lyddane–Sachs–Teller relation for a multimode crystal [15]:

$$\prod_{j=1}^{5}\frac{\omega_{\mathrm{LO},j}^2}{\omega_{\mathrm{TO},j}^2}=\frac{\varepsilon_0}{\varepsilon_{\mathrm{opt}}} \tag{3}$$

Here ε_0 and $\varepsilon_{\mathrm{opt}}$ are the dielectric constants including and excluding the excitation of one-phonon modes, i.e. below and above the phonon frequencies, respectively. Since we know all quantities appearing in Eq. (3), we can use this equation for a consistency check. The reasonable agreement between the value 4.5 ± 0.2 which we obtain for the left side from the phonon frequencies and the value 4.2 ± 0.3 which we calculate for the right side from the dielectric function, gives confidence in our evaluation of the data. From the phonon frequencies and the dielectric function in the transparent energy range $\varepsilon_{\mathrm{opt}}=n_{\mathrm{opt}}^2-k_{\mathrm{opt}}^2\approx n_{\mathrm{opt}}^2$ the sum over the squares of the effective charges of the ions e_i^{*2} can be calculated:

$$4\pi N\sum_i\frac{e_i^{*2}}{M_i}=\varepsilon_{\mathrm{opt}}\sum_j\left(\omega_{\mathrm{LO},j}^2-\omega_{\mathrm{TO},j}^2\right) \tag{4}$$

Here N is the number of unit cells in the unit volume, M_i is the mass of the ith ion and the sum extends over the ions in the unit cell. With the neutrality condition $e_{\mathrm{y}}^*+3e_{\mathrm{H}}^*=0$ Eq. (4) gives for the generalized Born effective charges $e_{\mathrm{Y}}^*=4.5\pm0.4$ and $e_{\mathrm{H}}^*=1.5\pm0.1$. The inclusion of the Lorentz correction for the internal field [13] transforms these values through the relation $e_{\mathrm{s},i}^*=[3/(\varepsilon_{\mathrm{opt}}+2)]e_i^*$ to the Szigeti effective charges $e_{\mathrm{s,Y}}^*=(1.4\pm0.2)e$ and $e_{\mathrm{s,H}}^*=(0.5\pm0.1)e$. This is considerably larger than the value of $0.29e$ derived for hydrogen from Y 3d core level shift experiments [16] and has the opposite sign to what has been claimed from soft X-ray emission and absorption measurements [17]. While the derivation from core level shifts suffers from the problem that the UHV required for the X-ray photoemission experiment may unload YH_3, the opposite sign derived from soft X-ray experiments appears to be due to the model chosen for the interpretation of the experimental data.

To appreciate our numbers for e_{S}^* a comparison with similar data for other materials is helpful. For NaCl, which is the prototype for ionic bonding, $0.74e$ are transferred from Na to Cl. For LiH, a hydride of an alkali metal, known for the formation of highly ionic compounds, the charge transfer to hydrogen is with $0.52e$ [18] very comparable to our result. Finally we cite GaAs, a rather covalent semiconductor with a nominally trivalent cation like yttrium. Here the transfer from Ga amounts to only $0.51e$ [18], i.e. it is nearly a factor three smaller than the transfer from Y in YH_3. This indicates that the bonding in YH_3 can be considered to be substantially ionic, a statement which is also supported by the energy gap of 2.8 eV [6], which exceeds largely the gap of $\approx$1.5 eV of GaAs.

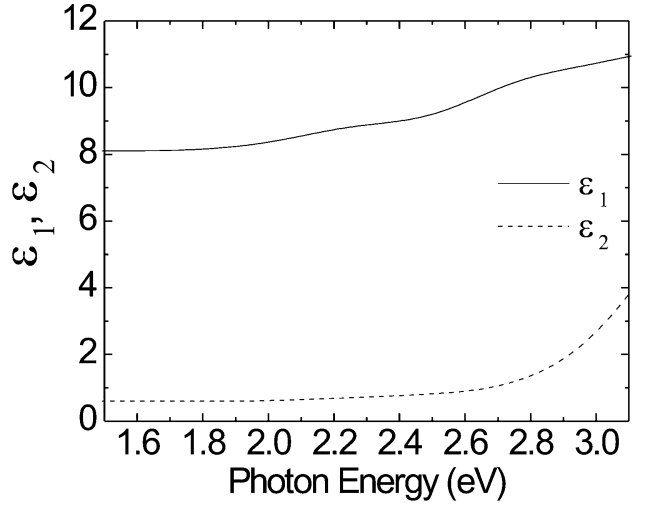

Fig. 5. Energy dependence of the real and imaginary part of the dielectric function of YH_3 as derived from the interference.

4. Raman scattering and crystal structure

Although the growth process for epitaxial yttrium films on CaF_2 and BaF_2 differs, both kinds of substrates are exposed to a temperature of 700 °C [11]. This creates defects leading to several weak and broad Raman lines, besides the typical narrow and strong Raman line for the cubic CaF_2 structure. As mentioned earlier, the micro-Raman technique allows to suppress weaker Raman lines coming from the substrates by a focusing of the laser beam onto the yttrium hydride film. Fig. 6 shows such spectra for YH_2 and YH_3 on an (111)-oriented CaF_2 substrate at room temperature. We observe in both spectra at 322 cm^{-1} the Raman-active phonon from the CaF_2 substrate through

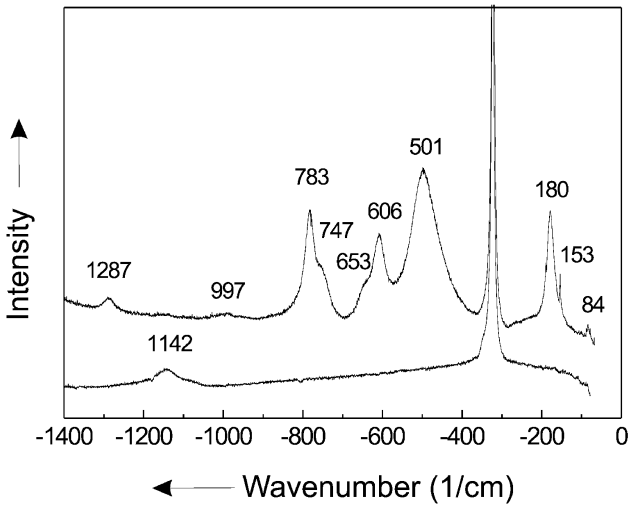

Fig. 6. Micro-Raman spectrum of YH_2 (bottom) and YH_3 (top) at room temperature.

which the measurement is performed. For YH_2 we find in addition one single line at 1142 cm^{-1}, which we associate with the Raman-active phonon of the CaF_2 structured YH_2. It is remarkable that the ratio of the wave numbers of these Raman-active modes in YH_2 and CaF_2 is with 3.54 within 0.7% of the square root of the reduced masses of the two compounds (i.e. equal within the experimental error). Since the Raman-active phonon mode in the CaF_2 structure (space group $Fm\underline{3}m$) corresponds to a vibration of the anions against the immobile cation, we expect from the masses a shift of the phonon frequencies by a factor given by the square root of the anion masses, i.e. by a factor $\sqrt{19}=4.36$. The agreement with the reduced masses must therefore be accidental. The larger effect of the masses is partly compensated by the force constant, which is reduced in YH_2 due to the free carriers which shield the charges of the ions. On substitution of deuterium for hydrogen the Raman-active mode shifts to 802 cm^{-1}, which is close to the factor $\sqrt{2}$, as expected from the mass ratio. The second curve in Fig. 6 displays the Raman spectrum for YH_3 at room temperature. One sees eight lines and two shoulders. The intensities are higher than for YH_2, reflecting the insulating nature of YH_3. When the temperature is lowered to 4 K the shoulders at 653 and 747 cm^{-1} develop to well resolved peaks and the broad line at 499 cm^{-1} splits into three structures. Thus one can identify 12 lines. With the exception of the three lines below 180 cm^{-1}, all lines are shifted by approximately $\sqrt{2}$ if hydrogen is replaced by deuterium [9]. This indicates that these low frequency lines involve vibrations of Y only, while the other nine lines correspond to vibrations including hydrogen, respectively deuterium. Table 1 collects the result of a factor-group analysis for the different structures which have either been assigned or have been proposed so far for Y, YH_2 and YH_3. While the single, twofold degenerate line for Y (at 88 cm^{-1}) and the threefold degenerate line for

Table 1
Factor-group analysis of Raman and IR-active phonons for the different structures under discussion for Y, YH_2 and YH_3

Material	Space group	Raman active modes	IR active modes
Y	$P6_3mmc$	E_{2g}	
YH_2	$Fm\underline{3}m$	F_{2g}	F_{1u}
YH_3	$P6_3mmc$	$A_{1g}+E_{1g}+2E_{2g}$	$2A_{2u}+2E_{2u}$
	$P\underline{3}c1$	$5A_{1g}+12E_g$	$6A_{2u}+11E_u$
	$P6_3cm$	$7A_1+11E_1+12E_2$	$7A_1+11E_1$
	$P6_3$	$11A_1+11E_1+12E_2$	$11A_1+11E_1$

YH_2 (at 1142 cm^{-1}) have been identified, the situation is significantly more complicated for YH_3. The $P6_3mmc$ structure was inferred from first X-ray scattering experiments [19] and was used for an early band structure calculation using the local density approximation (LDA) [20]. The first interpretation by Udovic et al. [21] of neutron scattering experiments stated that the structure was $P\underline{3}c1$. After some debate which was initiated by the result of LDA calculations indicating that a lowering of the symmetry would lead to the opening of a gap [22], the authors of the neutron experiments argued that their data could also be interpreted in terms of the $P6_3cm$ structure [23]. However, LDA theory finds the $P6_3$ structure to have the lowest energy [22]. As suggested by the increasing number of possible phonon modes in Table 1 the symmetry decreases for the quoted potential YH_3 structures from top to bottom. While in the $P6_3mmc$ structure hydrogen occupies two types of sites, namely tetrahedral and octahedral sites, the number of sites increases continuously from top to bottom to reach five different sites in the $P6_3$ structure. An other important difference is the presence of a center of inversion in the $P6_3mmc$ and $P\underline{3}c1$ structures and the absence of this center in the $P6_3cm$ and $P6_3$ structures. The same argument as for the IR data, that we observe more lines than predicted for the $P6_3mmc$ structure, applies also for the Raman spectra. Twelve lines are many more than the four lines predicted by group theory. But also the $P\underline{3}c1$ structure can be excluded by our Raman investigations. To do so, the polarization of the lines has been analyzed. As shown in Fig. 7, seven of the 12 lines disappear when the polarization is changed from parallel to perpendicular. This is a clear indication that these seven lines are A-type phonons, which is more than the five A_{1g} modes predicted by theory. It agrees with the number of modes for the $P6_3cm$ structure, making this structure most likely. However, on the basis of the number of modes only, one can not definitively exclude structures which would allow for more than the observed modes. One can not exclude that some of the predicted lines might be nearly degenerate or that some are too weak to be observed. A final remark needs to be made regarding the numbering of the Raman lines. In a previous paper the number of lines was 11 [9]. We have now identified two more lines, namely one line on the low energy side of our spectrum and one additional shoulder belonging to the broad peak around

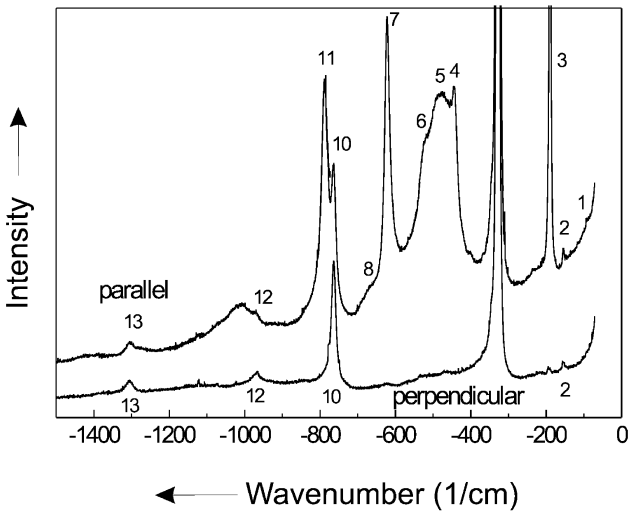

Fig. 7. Raman spectrum of YH_3 at 4 K for parallel and perpendicular polarization. Those lines which are only present for parallel polarization correspond to A-type phonons.

500 cm^{-1}. Line 9 at 730 cm^{-1} shows up when the sample is rotated out of normal incidence by 45°. The presence of this line indicates a E_1 type phonon, excluding once more the $P\underline{3}c1$ structure. A recent determination of electric field gradients in $YD_{2.98}$ using deuteron magnetic resonance corroborates our view, showing that the characteristic quadrupole frequencies and the asymmetry parameter agree much better with the space group $P6_3cm$ than $P\underline{3}c1$ [24].

5. Conclusions

We have reviewed quantitative IR and Raman studies of yttrium–hydride films. These methods are particularly powerful, since in contrast to X-ray or neutron scattering showing only weak interactions with light elements, lattice vibrations involving light elements have large energies giving large Raman shifts. Our IR data indicate that YH_3 is a substantially ionic compound. The number of IR-active phonon modes excludes the simple hexagonal ($P6_3mmc$) structure. Raman measurements exclude, in addition, the HoD_3 ($P\underline{3}c1$) structure. These observations and the fact that also cubic LaH_3 has a comparable optical gap [6] makes it hard to believe that the symmetry of the crystal structure plays an important role in the gap formation. It is more likely that correlation effects are responsible for the insulating nature of the trihydrides. Ng et al. [25] start from an ionic picture with an H^- ion and investigate the effect of the correlations on the width of the H^- band. They find that correlations reduce the LDA width of the H^- band of initially $\approx$10 eV by several eV leading to the opening of a gap of about 3 eV. In the correlation model of Eder et al. [26] the hopping integral depends on the occupation number of hydrogen and this introduces a correction of the hydrogen potential leading to a lowering of the H^- valence band. Although the mechanism of the gap opening is different in these two correlation models, the former relating it to a narrowing and the latter to a shift, both models involve a negatively charged hydrogen ion. This contrast with the recent GWA calculations [27,28] which arrive at a gap by a self-energy correction, but which essentially treat the trihydrides as covalent materials. Further investigations, like a precise study of the optical absorption below and at the gap energy, should allow to decide which description is closest to reality. At the moment we favor the correlated models, since the observed ionicity is a fundamental ingredient of these models.

Acknowledgements

The authors thank Drs. U. Barkow and A. Jacob for their contributions in an earlier stage of the investigations and to T. Lampe for technical assistance. The financial support of the European Commission through the TMR network ‘Switchable metal hydride films’ is acknowledged.

References

[1] B. Stalinski, Bull. Acad. Polon. Sci. 5 (1957) 997;
B. Stalinski, Bull. Acad. Polon. Sci. 5 (1957) 1001;
B. Stalinski, Bull. Acad. Polon. Sci. 7 (1959) 269.
[2] See for example G. Alefeld, J. Völkl (Eds.), Hydrogen in Metals I/II, Topics in Applied Physics, Vols. 28/29, Springer, Berlin, Heidelberg, New York, 1978.
[3] R. Bischof, E. Kaldis, P. Wachter, J. Magn. Magn. Mater. 31–34 (1983) 255.
[4] J.N. Huiberts, R. Griessen, J.H. Rector, R.J. Wijngaarden, J.P. Dekker, D.G. de Groot, N.J. Koeman, Nature (London) 380 (1996) 231.
[5] P. van der Sluis, M. Ouwerkerk, P.A. Duine, Appl. Phys. Lett. 70 (1997) 3356.
[6] A.T.M. van Gogh, D.G. Nagengast, E.S. Kooij, N.J. Koeman, J.H. Rector, R. Griessen, C.F.J. Flipse, R.J. Smeets, Phys. Rev. B 63 (2001) 195105.
[7] J. Schoenes, Optical and magneto-optical properties, in: A.J. Freeman, G.H. Lander (Eds.), Handbook on the Physics and Chemistry of the Actinides, Vol. 1, North Holland, Amsterdam, 1984, pp. 341–413.
[8] M. Rode, A. Borgschulte, A. Jacob, C. Stellmach, U. Barkow, J. Schoenes, Phys. Rev. Lett. 87 (2001) 235502.
[9] H. Kierey, M. Rode, A. Jacob, A. Borgschulte, J. Schoenes, Phys. Rev. B 63 (2001) 134109.
[10] D.C. Nagengast, J. Kerssemakers, A.T.M. van Gogh, B. Dam, R. Griessen, Appl. Phys. Lett. 75 (1999) 1724.
[11] A. Jacob, A. Borgschulte, J. Schoenes, Thin Solid Films 414 (2002) 39.
[12] A. Borgschulte, S. Weber, J. Schoenes, Appl. Phys. Lett., submitted for publication.
[13] P. Brüesch, Phonons: Theory and Experiments I, Springer, Berlin, 1982;
P. Brüesch, Phonons: Theory and Experiments II, Springer, Berlin, 1986.

[14] J. Schoenes, P. Brüesch, Solid State Commun. 38 (1981) 151.
[15] T. Kurosawa, J. Phys. Soc. Jpn. 16 (1961) 1298.
[16] J. Osterwalder, Z. Phys. B 61 (1985) 113.
[17] B. Hjörvarsson, J.-H. Guo, R. Ahuja, R.C.C. Ward, G. Andersson, E. Eriksson, M.R. Wells, C. Sathe, A. Agui, S.M. Butorin, J. Nordgren, J. Phys. Condens. Matter. 11 (1999) L119.
[18] E. Burnstein, in: T.A. Bak (Ed.), Phonons and Phonon Interactions, Benjamin, New York, 1964.
[19] C.E. Lunden, J.P. Blackledge, J. Electrochem. Soc. 109 (1962) 838.
[20] J.P. Dekker, J. van Ek, A. Lodder, J.N. Huiberts, J. Phys. Condens. Matter. 5 (1993) 4805.
[21] T.J. Udovic, Q. Huang, J.J. Rush, J. Phys. Chem. Solids 57 (1995) 423.
[22] P.J. Kelly, J.P. Dekker, R. Stumpf, Phys. Rev. Lett. 78 (1997) 1315.
[23] T.J. Udovic, Q. Huang, R.W. Erwin, B. Hjövarsson, R.C.C. Ward, Phys. Rev. B 61 (2000) 12701.
[24] O.J. Zogal, W. Wolf, P. Herzig, A.H. Vuorimäki, E.E. Ylinen, P. Vajda, Phys. Rev. B 64 (2001) 214110.
[25] K.K. Ng, F.C. Zhang, V.I. Anisimov, T.M. Rice, Phys. Rev. Lett. 78 (1997) 1311;
K.K. Ng, F.C. Zhang, V.I. Anisimov, T.M. Rice, Phys. Rev. B 61 (1999) 5398.
[26] R. Eder, H.F. Pen, G.A. Sawatzki, Phys. Rev. B 56 (1997) 19115.
[27] T. Miyake, F. Aryasetiawan, H. Kino, K. Terakura, Phys. Rev. B 61 (2000) 16491.
[28] P. van Gelderen, P.A. Bobbert, P.J. Kelly, G. Brooks, Phys. Rev. Lett. 85 (2000) 2989;
P. van Gelderen, P.A. Bobbert, P.J. Kelly, G. Brooks, Phys. Rev. B 66 (2002) 075104.